Bound states induced giant oscillations of the conductance in the quantum Hall regime

A. M. Kadigrobov[1] and M.V. Fistul[1,2]
[1] *Theoretische Physik III, Ruhr-Universität Bochum, D-44801 Bochum, Germany*
[2] *National University of Science and Technology MISIS, Moscow 119049, Russia*

(Dated: September 4, 2015)

We theoretically studied the quasiparticle transport in a 2D electron gas biased in the quantum Hall regime and in the presence of a lateral potential barrier. The lateral junction hosts the specific magnetic field dependent quasiparticle states highly localized in the transverse direction. The quantum tunnelling across the barrier provides a complex bands structure of a one-dimensional energy spectrum of these bound states, $\epsilon_n(p_y)$, where p_y is the electron momentum in the longitudinal direction y. Such a spectrum manifests itself by a large number of peaks and drops in the dependence of the magnetic edge states transmission coefficient $D(E)$ on the electron energy E. E.g., the high value of D occurs as soon as the electron energy E reaches gaps in the spectrum. These peaks and drops of $D(E)$ result in giant oscillations of the transverse conductance G_x with the magnetic field and/or the transport voltage. Our theoretical analysis based on the coherent macroscopic quantum superposition of the bound states and the magnetic edge states propagating along the system boundaries, is in a good accord with the experimental observations found in Ref.[1]

PACS numbers: 75.47.-m,03.65.Ge,05.60.Gg,75.45.+j

Great interest has been devoted to theoretical and experimental studies of various low-dimensional systems such as tunnel junctions, quantum point contacts (QPC), quantum nanowires, and 2D electron gas based nanostructures, just to name a few. These systems show a large variety of fascinating quantum-mechanical effects on the macroscopic scale, e.g. the weak localization[2,3], the quantum Hall effect[4], the macroscopic quantum tunnelling[5], the conductance quantization in QPCs[2,4,6] etc.

The quantum-mechanical dynamics of quasiparticles and the electronic transport become even more complex and intriguing when *bound states* are present in such systems. Indeed, it was shown in Ref.[7,8] that the bound states manifest themselves by narrow drops (the anti-resonance) in the gate voltage dependent conductance of QPCs. It is well known also that the bound states naturally arising on the boundaries of various systems such as graphene nanoribbons[9], nanowires[10,11], 2D electron gas under magnetic field, greatly influence the transport properties.

Specific magnetic field dependent bound states can be artificially created if a lateral junction (barrier) is fabricated inside of a 2D electron gas subject to an externally applied magnetic field (see Fig. 1)[1,12–15]. These highly localized states are formed due to the quantum-mechanical interference of magnetic edge states occurring on the both sides of the barrier. The localization length in the transverse direction x is of the order of the magnetic length $\ell_c \simeq \sqrt{\hbar c/(eH)}$ in the regime of a strong externally applied magnetic field, H.

However, in the longitudinal direction y these states show delocalized behavior, and the dynamics of electrons is characterized by the component of electron momentum p_y. Thus, in such a 1D channel the energy spectrum of electrons, $\epsilon_n(p_y)$, contains many bands, and it is shown for two lowest bands in Fig. 2A. In the absence

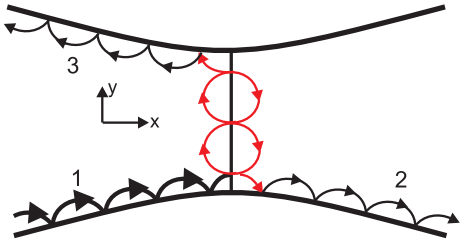

FIG. 1: **The point contact with a lateral junction in the quantum Hall regime.** A scattering process (propagation and reflection) of magnetic edge states on the electron states localized on the lateral junction, is schematically shown.

of quantum tunnelling across the junction the left-right symmetry of the electron states results in a large number of degenerate states in the electronic spectrum (see Fig. 2A, dashed line). The quantum tunnelling provides the lifting of the degeneracy, and the energy spectrum shows a complex structure with bands and gaps (see Fig. 2A, solid line). Notice here that in the region of a rather small magnetic field such a spectrum was calculated in Ref.[13,14], and in the region of a strong magnetic field, i.e in the quantum Hall regime, it was obtained in Ref.[1]. Since this spectrum having an origin in the coherent quantum-interference phenomenon, is extremely sensitive to various interacting effects, the renormalization of the above-mentioned spectrum due to the Coulomb interaction and /or the impurities has been theoretically studied in papers[16–20].

The bands and gaps in the energy spectrum of electronic states bounded to the junction, directly manifest themselves in a large amount of interesting effects as the transport in the longitudinal direction is studied. Indeed, the giant oscillations of the longitudinal conductance with the gate voltage, strongly nonlinear current-voltage characteristics and coherent Bloch oscillations

under a weak electric fields, have been predicted and theoretically studied[13,14].

It is naturally to suppose that the above-mentioned unique electronic spectrum can be probed by the electric current flowing *across* a lateral junction. In this article we show that the bands and gaps in the quasiparticle spectrum of the states bounded to a lateral junction, manifest themselves in giant oscillations of the conductance G_x as the applied magnetic field or dc voltage are varied. The origin of these oscillations is in the magnetic edge states transmission coefficient $D(E)$ which shows peaks and drops as the electron energy is tuned.

Qualitatively, the quantum-mechanical dynamics of electrons in a strong magnetic field and in the presence of a lateral junction can be considered as following: the lateral junction serves as a tunable quantum-mechanical scatterer for propagating edge states (see Fig. 1). E.g., the edge state 1 propagating from the left lead along the lower boundary is scattered by the barrier into the edge state 2 going to the right lead, and into the edge state 3 which reflects from the barrier to the left lead along the upper boundary. The highest probability of such reflection occurs if the propagation of electrons *along* the junction is allowed. It takes place if the electron energy E is inside of the energy bands of bound states. In this case the transmission coefficient $D(E)$ shows minimal values. As the energy of electrons is tuned to gaps in the spectrum of the bound states, the edge states propagation along the junction is forbidden, and a great enhancement of $D(E)$ is obtained. These oscillations of $D(E)$ transform in giant oscillations of G_x under variation of the magnetic field or the dc voltage. Such oscillations of G_x have been verified experimentally in the Ref.[1] but the quantitative analysis has not been done. Notice here, that in the Ref.[21], the electron current flowing perpendicular to the lateral junction in a 2D electron gas under a strong magnetic filed was numerically calculated, and similar oscillations of the conductance were obtained.

Below we present a complete analytical solution of the transverse transport of electrons in such a system that allows to clarify both qualitatively and quantitatively experimental features[1] such as the small value of the observed conductance in comparison to the expected Landauer conductance, the oscillations of the conductance as a function of the magnetic field or voltage, the dependence of the conductance on the lateral size of the system, etc. Our analysis based on the quantum-mechanical scattering of propagating magnetic edge states on the bound states is in a good accord with both the qualitative scenario and experimental observations.

Let us consider a QPC fabricated in a two-dimensional electron gas in the presence of a lateral junction and subject to an externally applied magnetic field. The magnetic field H is perpendicular to the QPC plane. The QPC is characterized by the coordinate-dependent electrostatic potential $\widetilde{V}(x,y) = \frac{m\omega_1^2}{2}y^2 + V(x)$, where the last term describes the potential barrier between two parts of the electron gas. The parameter ω_1 characterizes the curvature of the confinement potential of the QPC, m is the electron effective mass.

Quantum dynamics of electrons in the QPC with the lateral junction is described by the wave function $\Psi(x,y)$ satisfying the two-dimensional Schrödinger equation:

$$-\frac{\hbar^2}{2m}\frac{\partial^2\Psi}{\partial x^2} + \Big[\frac{1}{2m}\big(-i\hbar\frac{\partial}{\partial y} - \frac{eHx}{c}\big)^2 + \frac{m\omega_1^2}{2}y^2 + V(x) - E\Big]\Psi = 0, \quad (1)$$

where the Landau gauge, i.e. the vector-potential $\mathbf{A} = (0, Hx, 0)$, is used. Here, the axis y is parallel to the barrier and the x-axis is directed along the QPC (see Fig. 1). Introducing the dimensionless variables, $\xi = x/\ell_c$ and $\varepsilon = E/(\hbar\omega_c)$ (the ω_c is the cyclotron frequency), we write the total wave function Ψ as

$$\Psi(\xi,y) = \int_{-\infty}^{\infty} Q(p_y,\xi)\exp\{i\frac{p_y y}{\hbar}\}dp_y,$$
$$Q(p_y,\xi) = \sum_{n=0}^{\infty} R_n(p_y)\varphi_{n,p_y}(\xi) \quad (2)$$

Here, the partial wave functions $\varphi_{n,p_y}(\xi)$ describe the magnetic field dependent electron states bounded to the lateral junction and satisfy to the equation

$$\frac{\partial^2\varphi_{n,p_y}}{\partial\xi^2} - \Big[\Big(\frac{p_y\ell_c}{\hbar} - \xi\Big)^2 + \nu(\xi) - 2\varepsilon_n(p_y)\Big]\varphi_{n,p_y}(\xi) = 0 \quad (3)$$

with the boundary conditions being $\varphi_{n,p_y}(\xi) \to 0$ at $\xi \to \pm\infty$. Here, the dimensionless potential of the junction is $\nu(\xi) = 2mV(\xi l_c)\ell_c^2/\hbar^2$. These bound states are formed from the edge states propagating along the barrier $\phi^{(l)}_{n,p_y}(\xi)$ ($\phi^{(r)}_{n,p_y}(\xi)$) on the left (right) parts of the lateral junction. In the quantum Hall regime as $E \simeq \hbar\omega_c$ these bound states decay in the transverse direction on the distance ℓ_c. In the absence of quantum tunneling the electronic spectrum contains a large amount of degenerate states. The quantum-mechanical interference between left and right edge states results in a lifting of this degeneracy, and a peculiar one-dimensional spectrum $\varepsilon_n(p_y)$ with an alternating sequence of narrow energy bands $\sim \sqrt{1-|t|^2}\ \hbar\omega_c$ and energy gaps,[1,13,14] $\Delta_n \sim |t|\ \hbar\omega_c$, where $|t|^2$ is the barrier transparency (see Fig. 2A).

The transverse electronic transport is determined by the partial wave functions $R_n(p_y)$ which, in turn, are entangled with the bound states. Next, we explicitly consider this quantum entanglement in the case that the energy of electrons is in the vicinity of the first "crossing point". This crossing point occurs at $p_y = 0$, and the energy $\epsilon_0 = 3/2$ (in dimensionless units).

The generic total quantum-mechanical state is presented as a superposition of basis functions, i.e.

$$Q_0(p_y,\xi) = C_1(\varepsilon)R_0^{(l)}(p_y)\phi^{(l)}_{0,p_y}(\xi) + C_2(\varepsilon)R_0^{(r)}(p_y)\phi^{(r)}_{0,p_y}(\xi) \quad (4)$$

Here, $R_0^{(l,r)} = R_0 \pm R_1$ are the functions normalized to the unit flux density, the energy dependent coefficients

$C_1(\varepsilon)$ and $C_2(\varepsilon)$ determine the transmission coefficient $D(E)$ and, therefore, the electronic transport.

The partial wave functions $R_0^{(l,r)}(p_y)$ are satisfied to the following set of coupled equations (its derivation is given in Supplementary Materials):

$$\left(\frac{\alpha^2}{2}\frac{\hbar^2}{\ell_c^2}\frac{d^2}{dp_y^2}+\varepsilon_0^{(l)}(p_y)-\varepsilon\right)R_0^{(l)}+\tilde{\Delta}R_0^{(r)}=0;$$
$$\left(\frac{\alpha^2}{2}\frac{\hbar^2}{\ell_c^2}\frac{d^2}{dp_y^2}+\varepsilon_0^{(r)}(p_y)-\varepsilon\right)R_0^{(r)}+\tilde{\Delta}R_0^{(l)}=0, \quad (5)$$

where $\alpha=\omega_1/\omega_c$, and $\varepsilon_0^{(l,r)}(p_y)$ are the energy spectrum of the left(right) edge states in the absence of tunneling (dashed line in Fig. 2A), the dimensionless energy gap $\tilde{\Delta}=\Delta/(\hbar\omega_c)$ is determined by the quantum tunneling across the barrier.

As $\alpha \ll 1$ one may solve this set of equations in the quasiclassical approximation. Indeed, substituting $\Psi_{1,2}=A_{1,2}(p_y)\exp\{iS(p_y)\ell_c/(\hbar\alpha)\}$ in Eq.(A8) and introducing the classical momentum as $P=dS/dp_y$ one finds that the electron dynamics is determined by the quasiclassical phase trajectories $P(p_y)$ as

$$P^2=\varepsilon-\frac{\varepsilon_0^{(l)}(p_y)+\varepsilon_0^{(r)}(p_y)}{2}\pm$$
$$\pm\sqrt{\left(\frac{\varepsilon_0^{(l)}(p_y)-\varepsilon_0^{(r)}(p_y)}{2}\right)^2+\tilde{\Delta}^2}. \quad (6)$$

Notice here that the quasiclassical approximation is valid as $|\varepsilon-\varepsilon_0^{(l,r)}(p_y)|\gg\alpha^{2/3}$.

The quasiclassical phase trajectories determined by Eq.(6) for different values of the electron energy ε are shown in Fig. 2B. As the well separated phase trajectories approach to each other the quantum tunneling occurs between them. However, in contrast to the standard interband transitions[22], in the case under consideration the tunnelling takes place in the vicinity of Lifshitz's phase transition[23]. Indeed, as it follows from Eq.(6) there are two critical energies at which the topology of trajectories changes: at first, in the vicinity of the energy $\varepsilon_{cr}^{(1)}=\varepsilon_0-\tilde{\Delta}$ the mutual directions of the motion on two open trajectories vary (see Fig. 2Ba and 2Bb); secondly, a new closed orbit arises at the critical energy $\varepsilon_{cr}^{(2)}=\epsilon_0+\tilde{\Delta}$ (see Fig. 2Bc and 2Bd). The quasiclassical approximation breaks down not only at the turning points but also in the vicinity of the point $p_y=0$ where the quantum tunneling takes place.

In order to properly elaborate quantum tunnelling between various quasiclassical phase trajectories we apply the perturbation analysis which is valid in a whole ranges of energies but the energy gap $\tilde{\Delta}$ is assumed to be small. Introducing the Fourier transformation as

$$\Phi(p_y)_{1,2}=\int_{-\infty}^{\infty}g_{1,2}(Y)\exp\{i\frac{Yp_y\ell_c}{\hbar\alpha}\}dY \quad (7)$$

and presenting the Fourier transform $g_{1,2}(Y)$ in the form

$$g_{1,2}=u_{1,2}(\zeta)e^{\{\pm i(\frac{2}{3}\zeta^3+2\eta\zeta)\}}, \quad (8)$$

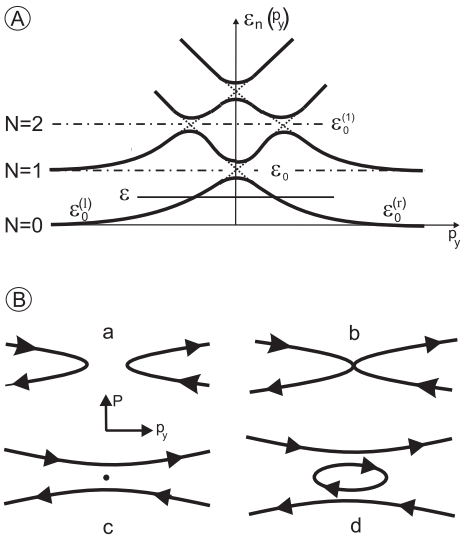

FIG. 2: **The energy spectrum of electron states bounded to the lateral junction and corresponding quasiclassical trajectories.** A) The lowest two bands of the spectrum $\epsilon_n(p_y)$ are shown by dashed (in the absence of tunneling) and solid (in the presence of tunneling) lines. B) The phase trajectories $P(p_y)$ for different values of the electron energy: a)$\varepsilon<\varepsilon_{cr}^{(1)}=\varepsilon_0-\tilde{\Delta}$; b)$\varepsilon=\varepsilon_{cr}^{(1)}$; c) $\varepsilon=\varepsilon_{cr}^{(2)}=\varepsilon_0+\tilde{\Delta}$; d)$\varepsilon>\varepsilon_{cr}^{(2)}$ (here $2\tilde{\Delta}$ is the energy gap).

one gets the following set of equations[24] for the new variable $\zeta=Y[\frac{\ell_c\omega_c}{\alpha v}]^{1/3}$ (here, $v=|d\varepsilon_0^{(l)}(p_y)/dp_y|$ is the electron velocity):

$$i\frac{du_1(\zeta)}{d\zeta}=-\gamma e^{-i\left(\frac{2}{3}\zeta^3+2\eta\zeta\right)}u_2(\zeta)$$
$$i\frac{du_2(\zeta)}{d\zeta}=+\gamma e^{i\left(\frac{2}{3}\zeta^3+2\eta\zeta\right)}u_1(\zeta), \quad (9)$$

where the parameters

$$\gamma=2^{1/3}\tilde{\Delta}\left[\frac{\ell_c\omega_c}{\alpha v}\right]^{2/3}, \quad \eta=2^{1/3}(\varepsilon_0-\varepsilon)\left[\frac{\ell_c\omega_c}{\alpha v}\right]^{2/3}. \quad (10)$$

Here, the parameter η controls the topology of the phase trajectories (see Fig.5B) and the parameter γ determines the probability of quantum tunnelling between trajectories.

The perturbation analysis of Eq.(9) in the limit of $\gamma\ll 1$ allows one to obtain the probability $D(E)$ for a particle in the momentum space to be transmitted from $p_y\to+\infty$ to $p_y\to-\infty$ as

$$D(\epsilon)=\gamma^2\left[\pi 2^{2/3}\mathrm{Ai}\left(2^{2/3}\eta\right)\right]^2, \quad (11)$$

where $\mathrm{Ai}(x)$ is the Airy function[27] (see Supplementary Material, Section II). The typical dependence of $D(\epsilon)$ is shown in Fig. 3.

One can see that $D(E)$ is an extremely small as $E<(3/2)\hbar\omega_c$. In the opposite regime at $E>(3/2)\hbar\omega_c$, $D(E)$

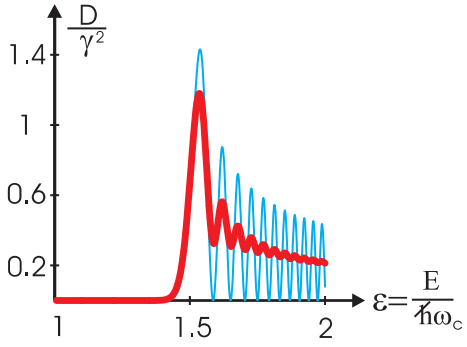

FIG. 3: **Energy dependent transmission probability.** Dependence of the transmission probability D on the normalized energy ε is shown. The transparency of the lateral barrier (which acts as a tunable quantum scatterer) is zero as long as the electron energy is below the lowest energy gap at $E_0/\hbar\omega_c = 1.5$ (see Fig. 5A). Further increase of E results in a narrow sharp peak accompanied by fast transparency oscillations (thin solid line) caused by the quantum interference inside the effective scatter. The fast oscillations are partially washed out at finite temperature T (thick solid line). The parameters $\alpha = 10^{-2}$, $v/(l_c\omega_c) = 2$, and $k_BT/\hbar\omega_c = 10^{-2}$ have been used.

displays both a great enhancement and fast oscillations with a small period of $\delta E_1 \simeq \hbar\omega_c\alpha^{2/3}$. The origin of these oscillations is the quantization of a quantum-mechanical phase of the wave function of electrons moving along the closed orbit (see, Fig. 2Bd). At finite temperatures these fast oscillations are partially washed out, and it results in a strong decay of the function $D(E)$ as $E > (3/2)\hbar\omega_c$ (see Fig. 3, thick solid line).

As we turn to the electronic transport in the quantum Hall regime it can be shown (see Supplementary Material, for details) that $D(E)$ determines also the energy dependent transmission coefficient of electrons propagating across the lateral junction. Thus, $D(\mu)$ determines the linear conductance G_x. Here, μ is the chemical potential of the system.

The current-voltage characteristic $I(V)$ of the QPC in a broad voltage region is obtained by making use of the Landauer-Büttiker approach[4] as:

$$I(V) = \frac{2e}{h}\sum_n \int dE D_n(E) \qquad (12)$$
$$[f(E+eV/2) - f(E-eV/2)]\ ,$$

where $f(E)$ is the Fermi-Dirac distribution function. Notice here, that the transmission coefficients for upper bands, D_n, are also determined by the energy differences to the crossing points ε_n as

$$D_n = \gamma_n^2\Big[\pi 2^{2/3}\mathrm{Ai}\left(2^{2/3}\eta_n\right)\Big]^2$$

where

$$\eta_n \approx 2^{1/3}(\varepsilon_n - \varepsilon)[\frac{\ell_c\omega_c}{\alpha v_n}]^{2/3}$$

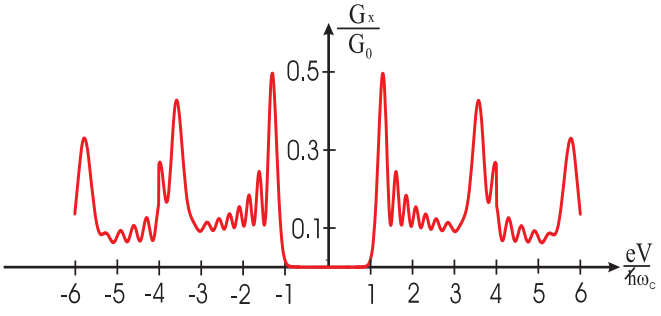

FIG. 4: **Dependence of the normalized conductance on the applied dc voltage.** The parameters $\alpha = 10^{-2}$, $\mu_0/\hbar\omega_c = 1$, $v/l_c\omega_c = 2$ and $k_BT/\hbar\omega_c = 10^{-2}$ have been used (here $G_0 = (4e/h)\gamma^2$ and μ_0 is the chemical potential in the absence of the applied voltage).

and

$$\gamma_n \approx 2^{1/3}\Delta_n\Big[\frac{\ell_c\omega_c}{\alpha v_n}\Big]^{2/3}$$

(see Supplementary Materials, Section III, for details) . The differential conductance G_x is determined as $G_x = dI/dV$. The typical dependence of $G_x(V)$ determined by Eqs. (11) and (C11) is shown in Fig. 4.

The dependence of $G_x(V)$ displays giant oscillations with the period $\delta E_2 \simeq \hbar\omega_c$. The two reasons determine the appearance of peaks in the $G_x(V)$ dependence: at first, the applied voltage distorts the spectrum of bound states to $\epsilon_n(p_y, eV)$, and secondly, the voltage tunable energy of electrons $E = \mu + eV/2$ traces the energy gaps Δ_n in the spectrum of bound states.

The consistent experimental study of the conductance of a 2D electron gas biased in the quantum Hall regime and in the presence of a lateral junction has been carried out in Ref.[1]. Our quantitative analysis presented in Fig. 3,4 shows all important features observed in[1], namely a great enhancement and fast oscillations of the linear conductance $G_x(0)$ as the magnetic field was decreased (a decrease of the magnetic field results in an effective increase of the chemical potential μ), and unique giant oscillations of $G_x(V)$.

In conclusion, we have shown that in the quantum Hall regime a lateral junction formed in the QPC serves as a unique quantum-mechanical scatterer for propagating magnetic edge states. Such a lateral junction hosts the electrons bound states having a peculiar magnetic field dependent 1D spectrum $\varepsilon_n(p_y)$. This spectrum contains an alternating sequence of narrow energy bands and gaps. These band and gaps manifests themselves by giant oscillations of the transmission coefficient $T(E)$ on the electron energy E and the voltage dependent conductance $G_x(V)$. Our theoretical analysis based on the coherent quantum-mechanical superposition of localized and delocalized magnetic edge states is in a good accord with the experemental observations[1]. Such a generic approach [see the Eqs. (A8) and (11)] can be applied to the variety of

solid state systems where the physical properties are determined by the coherent quantum dynamics of interacting quantum-mechanical objects, e.g. the magnetic edge states propagation in graphene based nanostructures[15] or the superconducting quantum metamaterials[28].

Acknowledgements: The financial support of the Ministry of Education and Science of the Russian Federation in the framework of Increase Competitiveness Program of NUST "MISiS"($K2-2014-015$) and the SPP programme "Graphene" of the DFG are acknowledged.

[1] W. Kang, H.L. Stormer, L.N. Pfeifer, K.W. Baldwin, and K.W. West, Letters to Nature, **403**, 59 (2000).
[2] Th. Heinzel, Mesoscopic Electronics in Solid State Nanostructures, Wiley-VCH (2003).
[3] W. Zwerger, *Theory of Coherent Transport* in Th. Dittrich, G-L. Ingold, G. Schön, P. Hänggi, B. Kramer, and W. Zwerger, *Quantum Transport and Dissipation*, Wiley-VCH (1998).
[4] B. Kramer, *Quantization of Transport*, in Th. Dittrich, G-L. Ingold, G. Schön, P. Hänggi, B. Kramer, and W. Zwerger, *Quantum Transport and Dissipation*, Wiley-VCH (1998).
[5] M. H. Devoret , J. M. Martinis, and J. Clarke, Phys. Rev. Lett. 55 1908 (1985); J. M. Martinis, M. H. Devoret, and J. Clarke, Phys. Rev. B 35, 4682 (1987).
[6] C. W. J. Beenakker and H. van Houten, Solid State Physics, 44 1 (1991).
[7] J. Masek and B. Kramer, Z. Phys. B **75**, 37 (1989).
[8] J.U. Nöckel and A. D. Stone, Phys. Rev. B **50**, 17415 (1994).
[9] A. H. Castro Neto, F. Guinea, N. M. R. Peres, K. S. Novoselov, and A. K. Geim, Rev. Mod. Phys. 81, 109 (2009).
[10] J.-C. Charlier, X. Blase, and S. Roche, Rev. Mod. Phys. 79, 677 (2007).
[11] V. Mourik, K. Zuo, S. M. Frolov, S. R. Plissard, E. P. A. M. Bakkers, and L. P. Kouwenhoven, Science 336, 1003 (2012).
[12] C. C. Eugster, J. A. del Alamo, M. J. Rooks, and M. R. Melloch, Appl. Phys. Lett. **64**, 3157 (1994);
[13] A.M. Kadigrobov, and I.V. Koshkin, Sov. J. low temp. Phys. **12**, 249 (1986).
[14] A.M. Kadigrobov, M.V. Fistul, and K.B. Efetov, Phys. Rev. B **73**, 235313 (2006).
[15] B. Özyilmaz, P. Jarillo-Herrero, D. Efetov, D. A. Abanin, L. S. Levitov, and Ph. Kim Phys. Rev. Lett. *99*, 166804 (2007).
[16] A. Mitra and S. M. Girvin, PRB **64**, 041309(R) (2001).
[17] M. Kollar, and S. Sachdev, Phys. Rev. B. **65**, 121304 (2002)
[18] S. Nonoyama and G. Kirczenow Physica E **18**, 120 (2003)
[19] E.-A. Kim and E. Fradkin, Phys. Rev. Lett. **91**, 156801 (2003)
[20] M. Aranzana, N. Regnault, and Th. Jolicoeur PRB **72**, 085318 (2005).
[21] Y. Takagaki and K.H. Ploog, PRB **62**,3766 (2000).
[22] E. O. Kane and E. I. Blount, in *Tunneling Phenomena in Solids*, edited by E. Burstein and S. Lundqvist (Plenum Press, New York, 1969)
[23] I. M. Lifshitz, Sov. Phys. JETP **11**, 1130 (1960).
[24] An analogous equation defines the magnetic breakdown probability near the touching points of classical orbits of an electron under a strong magnetic field[25].
[25] A.M. Kadigrobov, A. Bjelish, and D. Radić, Eur. Phys. J. B **86**, 276 (2013), Physica B, **460**,248 (2015).
[26] T. Ditrich *et al.*, "Quantum Transport and Dissipation", WILEY-VCH Verlag GmbH, Weinheim, Germany (1998).
[27] *Handbook of Mathematical Functions with Formulas, Graphs, and Mathematical Tables*, edited by M. Abramowitz and I.?A. Stegun (Dover, New York, 1972), 9th printing.
[28] P. Macha, G. Oelsner, J.-M. Reiner, M. Marthaler, St. Andre, Gerd Schön, U. Huebner, H.-G. Meyer, E. Il'ichev, and A. V. Ustinov, Implementation of a Quantum Metamaterial, *Nat. Commun.* **5**, 5146 (2014).

Supplementary Information

Appendix A: Derivation of Eq.(5) of the main text.

In this section we find the differential equation that describes dynamics of electrons in the vicinity of the points of degeneration of the left and right edge states travelling along the lateral barrier placed across the point contact as is shown in Fig.1 of the main text.

Inserting Q of Eq.(2) of the main text into Eq.(1) we obtain the following equation:

$$\sum_{n=0}^{\infty}\Big\{R_n\Big[\frac{\partial^2}{\partial\xi^2}-\Big(\frac{p_y\ell_c}{\hbar}-\xi\Big)^2-\nu(\xi)\Big]\varphi_{n,p_y}(\xi)$$
$$+\Big[-\Big(\frac{\omega_1}{\omega_c}\Big)^2\frac{\hbar^2}{\ell_c^2}\frac{d^2R_n}{dp_y^2}-2\varepsilon R_n\Big]\varphi_{n,p_y}(\xi)\Big\}=0. \quad \text{(A1)}$$

Here $\varphi_{n,p_y}(\xi)$ are proper functions of the following Schrödinger's equation:

$$\frac{\partial^2\varphi_{n,p_y}}{\partial\xi^2}-\Big[\Big(\frac{p_y\ell_c}{\hbar}-\xi\Big)^2+\nu(\xi)-2\varepsilon_n(p_y)\Big]\varphi_{n,p_y}(\xi)=0, \quad \text{(A2)}$$

where $\varepsilon_n(p_y)$ is the proper energy and n is the Landau number, the boundary conditions being $\varphi_{n,p_y}(\xi)\to 0$ at $\xi\to\pm\infty$.

Eq.(A2) describes dynamics of electrons under magnetic field in the presence of a longitudinal potential barrier $\nu(\xi)$ but in the absence of any constriction in the

direction parallel to the barrier. This situation was considered in Refs.[? ? ?]. It was shown that far from the barrier, $|x| > 2R_L$ (here R_L is the Larmour radius), the electron spectrum ε_n is the standard discrete Landau spectrum. The situation drastically changes for electrons travelling along the barrier. In this case the quantum interference of the edge states situated on its both sides transforms the electron spectrum into an alternating series of narrow energy bands and gaps (see Fig.5). As a result, both dynamics and kinetics of electrons in such a system qualitatively change.

In this section we find the differential equations that describe evolution of functions $R_n(p_y)$ in the vicinity of the "crossing points" (e.g., one of them is at $p_y = 0$ and $\varepsilon = \varepsilon_0$, see Fig.5) where the quantum tunnelling of electrons through the lateral junction lifts the degeneracy in the electron spectrum. Here we follow Landau's method for finding energy levels in a double well potential[?].

In the limit of a low barrier transparency the wave functions $\varphi_{n,p_y}(\xi)$ and $\varphi_{n+1,p_y}(\xi)$ close to the "crossing points" are conveniently presented as a combination of the left $\phi^{(l)}_{n,p_y}(\xi)$ and right $\phi^{(r)}_{n',p_y}(\xi)$ independent edge states the proper energies of which intersect in the middle of the gap. These states are localized in the left well, $\xi < 0$, and the right one, $\xi > 0$, respectively, and hence one may write:

$$\varphi_{n,p_y}(\xi) \approx \frac{1}{\sqrt{2}}\big(\phi_{n,1}(\xi) + \phi_{n,2}(\xi)\big)$$
$$\varphi_{n+1,p_y}(\xi) \approx \frac{1}{\sqrt{2}}\big(\phi_{n,1}(\xi) - \phi_{n,2}(\xi)\big); \qquad \text{(A3)}$$

where $\phi_{n,1}(\xi) \equiv \phi^{(l)}_{n,p_y}(\xi)$ and $\phi_{n,2}(\xi) \equiv \phi^{(r)}_{n',p_y}(\xi)$ are the edge state wave functions which satisfy the following equations:

$$\Big\{\frac{\partial^2}{\partial\xi^2} - \Big(\frac{p_y\ell_c}{\hbar} - \xi\Big)^2 - \nu(\xi) + 2\overline{\varepsilon}^{(n)}_{1,2}(p_y)\Big\}\phi_{n,1,2}(\xi) = 0 \qquad \text{(A4)}$$

with the boundary conditions $\phi^{(n)}_1(\xi) \to 0$ on the both boundaries of the left well while $\phi^{(n)}_2(\xi) \to 0$ on the both boundaries of the right one. Here $\overline{\varepsilon}^{(n)}_{1,2}(p_y)$ are the energies of edge states (see, e.g.[3]) which degenerate at $p_y = p^n_y$. Four such points at $p_y = 0$, $p_y = p^{(I,II)}$, are shown in Fig.5.

Multiplying Eq.(A1) by $\phi_{n,1}(\xi)$ and integrating over p_y from $-\infty$ to a as well as by $\phi_{n,2}(\xi)$ and integrating from a to $+\infty$ one gets the following set of coupled equations

$$\sum_{\bar n=0}^{\infty}\Big[\phi_{n,1}(a)\varphi'_{\bar n,p_y}(a) - \phi'_{n,1}(a)\varphi_{\bar n,p_y}(a)\Big]R_{\bar n}(p_y)$$
$$+\Big[\overline{\varepsilon}^{(n)}_1(p_y) - \varepsilon - \frac{\hbar^2}{2\ell_c^2}\alpha^2\frac{d^2}{dp_y^2}\Big]$$
$$\times\sum_{\bar n=0}^{\infty}R_{\bar n}\int_{-\infty}^{a}\phi_{n,1}(\xi)\varphi_{n,p_y}(\xi)d\xi = 0;$$
$$\sum_{\bar n=0}^{\infty}\Big[-\phi_{n,2}(a)\varphi'_{\bar n,p_y}(a) + \phi'_{n,2}(a)\varphi_{\bar n,p_y}(a)\Big]R_{\bar n}(p_y)$$
$$+\Big[\overline{\varepsilon}^{(n)}_2(p_y) - \varepsilon - \frac{\hbar^2}{2\ell_c^2}\alpha^2\frac{d^2}{dp_y^2}\Big]$$
$$\times\sum_{\bar n=0}^{\infty}R_{\bar n}\int_{a}^{\infty}\phi_{n,2}(\xi)\varphi_{\bar n,p_y}(\xi)d\xi = 0; \qquad \text{(A5)}$$

Here a is the point inside of the barrier at which $\varphi'_{n,p_y}(a) = 0$ and $\alpha = \omega_1/\omega_c$ while $f'(\xi) \equiv df(\xi)/d\xi$.

As the edge state functions are orthogonal and normalized while $\varphi_{n,p_y}(\xi)$ are approximated by Eq.(A3) one finds

$$\sum_{\bar n=0}^{\infty}R_{\bar n}\int_{-\infty}^{a}\phi_{n,1}(\xi)\varphi_{\bar n,p_y}(\xi)d\xi = \frac{1}{\sqrt{2}}\Big(R_n(p_y) + R_{n+1}(p_y)\Big);$$
$$\sum_{\bar n=0}^{\infty}R_{\bar n}\int_{a}^{+\infty}\phi_{n,2}(\xi)\phi_{\bar n,p_y}(\xi)d\xi = \frac{1}{\sqrt{2}}\Big(R_n(p_y) - R_{n+1}(p_y)\Big), \qquad \text{(A6)}$$

and

$$\sum_{\bar n=0}^{\infty}\Big[\phi_{n,1,2}(a)\varphi'_{\bar n,p_y}(a) - \phi'_{n,1,2}(a)\varphi_{\bar n,p_y}(a)\Big]R_{\bar n}(p_y) \approx$$
$$-\phi'_{n,1,2}(a)\frac{\phi_{n,1}(a) + \phi_{n,2}(a)}{\sqrt{2}}\Big(R_n(p_y) \mp R_{n+1}(p_y)\Big) \qquad \text{(A7)}$$

Inserting Eqs.(A6,A7) in Eq.(A5) one gets the set of differential equations presented in the main text (Eq.(5)):

$$\Big(\alpha^2\frac{\hbar^2}{2\ell_c^2}\frac{d^2}{dp_y^2} + +\overline{\varepsilon}^{(l)}_n(p_y) - \varepsilon\Big)R^{(l)}_n + \tilde\Delta_n R^{(r)}_n = 0;$$
$$\Big(\alpha^2\frac{\hbar^2}{2\ell_c^2}\frac{d^2}{dp_y^2} + \overline{\varepsilon}^{(r)}_n(p_y) - \varepsilon\Big)R^{(l)}_n + \tilde\Delta_n R^{(l)}_n = 0, \qquad \text{(A8)}$$

Here $R^{(l,r)}_n = R_n \mp R_{n+1}$, and

$$\tilde\Delta_n = -\phi'_{n,1}(a)\frac{\phi_{n,1}(a) + \phi_{n,2}(a)}{\sqrt{2}} \qquad \text{(A9)}$$

is the normalized energy gap in the spectrum of the bound states. For the sake of simplicity, below we drop the subscript n assuming that all energy gaps are equal.

Using Eq.(A8) at $n = 0$ one obtains Eq.(5) of the main text.

Appendix B: Derivation of the probability $D(E)$ of the electron transmission from $p_y \to -\infty$ to $p_y \to +\infty$, Eq.(11) of the main text.

1 step. In subsection A we find the semiclassical solutions of Eq.(A8) and we show that the semiclassical approximation fails not only at the turning points but in narrow vicinities of the degenerate points as well where the interband quantum transitions between semiclassical trajectories (see Fig. 2B) takes place.

2 step. Therefore, before finding the probability for an electron to pass from $p_y = -\infty$ to $p_y = +\infty$, we solve Eq.(A8) in the vicinity of the degeneration points developing some perturbation theory, see subsection B. We also show that there are regions on the both sides of the degeneration points where this solution overlaps with the semiclassical wave functions found in subsection A. The found solution allows to re-write it in terms of the probability transitions between these regions of the overlap, this probability $D(E)$ being the same as presented in Eq.(11) of the main text.

3 step. In subsection C, in order to prove that $D(E)$ is also the probability for the electron to pass from $p_y = -\infty$ to $p_y = +\infty$ we match the semiclassical wave functions and the perturbation ones in the regions of overlapping, and then we take asymptotic of the former functions at $p_y = \pm\infty$ and find Eq.(11) of the main text.

1. Quasiclassical wave function in the momentum space.

Here we find quasiclassical solutions of Eq.(A8) using the inequality $\alpha \ll 1$.

Presenting functions $R_n^{(l,r)}$ in the quasiclassical form

$$R_n^{(l,r)}(p_y) = A_n^{(l,r)}(p_y)\exp\{i\frac{S_n(p_y)\ell_c}{\hbar\alpha}\} \tag{B1}$$

one easily finds the classical momentum $P_n = dS_n/dp_y$, the semiclassical parameter κ

$$P_n^2 = \varepsilon - \frac{\overline{\varepsilon}_n^{(l)}(p_y) + \overline{\varepsilon}_n^{(r)}(p_y)}{2} \pm \sqrt{\left(\frac{\overline{\varepsilon}_n^{(l)}(p_y) - \overline{\varepsilon}_n^{(r)}(p_y)}{2}\right)^2 + \tilde{\Delta}^2};$$
$$\kappa = (\frac{\omega_c\ell_c}{\alpha v})^{2/3}|\varepsilon - \overline{\varepsilon}_n^{(l,r)}(p_y)| \gg 1 \tag{B2}$$

and the wave functions:

$$R_n^{(l)}(p_y)(p_y) = \frac{1}{(\varepsilon - \overline{\varepsilon}_n^{(l)})^{1/4}} \times\Big[B_1^{(n)}\exp\left(\frac{i\ell_c}{\hbar\alpha}\int^{p_y} P_1^{(n)}dp_y'\right) + B_2^{(n)}\exp\left(-\frac{i\ell_c}{\hbar\alpha}\int^{p_y} P_1^{(n)}dp_y'\right)\Big] + \frac{\tilde{\Delta}}{\overline{\varepsilon}_n^{(r)} - \overline{\varepsilon}_n^{(l)}} \times \frac{1}{(\varepsilon - \overline{\varepsilon}_n^{(r)})^{1/4}} \times\Big[C_1^{(n)}\exp\left(\frac{i\ell_c}{\hbar\alpha}\int^{p_y} P_2^{(n)}dp_y'\right) + C_2^{(n)}\exp\left(-\frac{i\ell_c}{\hbar\alpha}\int^{p_y} P_2^{(n)}dp_y'\right)\Big] \tag{B3}$$

$$R_n^{(r)}(p_y)(p_y) = -\frac{\tilde{\Delta}}{\overline{\varepsilon}_n^{(r)} - \overline{\varepsilon}_n^{(l)}} \times \frac{1}{(\varepsilon - \overline{\varepsilon}_1^{(n)})^{1/4}} \times\Big[B_1^{(n)}\exp\left(\frac{i\ell_c}{\alpha\hbar}\int^{p_y} P_1^{(n)}dp_y'\right) + \Big(B_2^{(n)}\exp\left(-\frac{i\ell_c}{\alpha\hbar}\int^{p_y} P_1^{(n)}dp_y'\right)\Big] + \frac{1}{(\varepsilon - \overline{\varepsilon}_n^{(r)})^{1/4}} \times\Big[C_1^{(n)}\exp\left(\frac{i\ell_c}{\alpha\hbar}\int^{p_y} P_2^{(n)}dp_y'\right) + \Big(C_2^{(n)}\exp\left(-\frac{i\ell_c}{\alpha\hbar}\int^{p_y} P_2^{(n)}dp_y'\right)\Big] \tag{B4}$$

where $B_{1,2}^{(n)}$ and $C_{1,2}^{(n)}$ are arbitrary constants, $P_{1,2}^{(n)}$ are two solutions of Eq.(B2) corresponding to $\pm$ at the squire root.

Quasiclassical trajectories $P_n = P_n(p_y;\varepsilon)$ corresponding to Eq.(B2) for two electron energies above the first energy gap (the Landau number $n = 0$) and above the next two ones (the Landau number $n = 1$) are shown in Fig.5b.

As one sees from Eqs.(B3,B4) the quasiclassical approximation fails not only at the turning point but at any degeneration point $p_y^{(n)}$ at which $\overline{\varepsilon}_n^{(l)}(p_y) = \overline{\varepsilon}_n^{(r)}(p_y)$. In the next section, in order to match the semiclassical wave functions we solve Eq.(A8) in the vicinity of the crossing points by making use of the perturbation analysis .

2. Derivation of the transfer matrix in the vicinity of a degeneration point.

We start derivation of the transfer matrix solving Eq.(A8) in the immediate vicinity of a degenerate point. Expanding the edge state energies $\overline{\varepsilon}_n^{(l,r)}(p_y) \approx \varepsilon_0^{(n)} \mp v_n^{(l,r)}\widetilde{p}_y$ (for the sake of certainty these signs of the edge

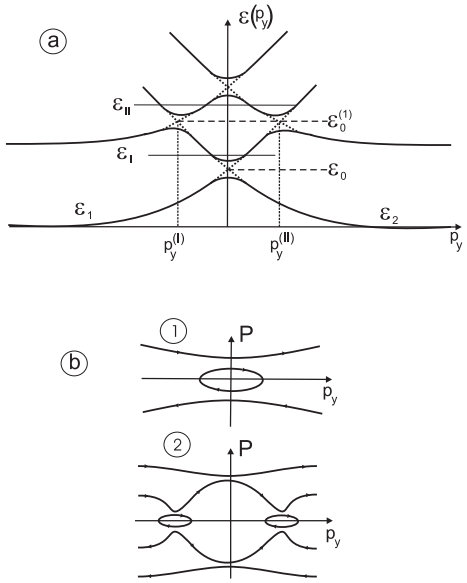

FIG. 5: a) Energy spectrum of the quasiparticles localized around the longitudinal barrier; bI and bII - semiclassical trajectories $P = P(p_y;\varepsilon)$ corresponding to $\varepsilon = \varepsilon_I$ and $\varepsilon = \varepsilon_{II}$, respectively.

state velocities are chosen to correspond to degeneration points $p_y^{(n)} \le 0$, see Fig.5, $\widetilde{p}_y = p_y - p_y^{(n)}$) one obtains the following equations:

$$\left(\alpha^2\frac{\hbar^2}{2\ell_c^2}\frac{d^2}{d\widetilde{p}_y^2} + \varepsilon - \varepsilon_0^{(n)} - v_n^{(l)}\widetilde{p}_y\right)R_n^{(l)} - \tilde{\Delta}R_n^{(r)} = 0;$$
$$\left(\alpha^2\frac{\hbar^2}{2\ell_c^2}\frac{d^2}{d\widetilde{p}_y^2} + \varepsilon - \varepsilon_0^{(n)} + v_n^{(r)}\widetilde{p}_y\right)R_n^{(r)} - \tilde{\Delta}R_n^{(l)} = 0 \quad \text{(B5)}$$

where $v_n^{(l,r)} = |d\overline{\varepsilon}_n^{(l,r)}/dp_y|$ taken at $p_y = p_y^{(n)}$.

To reduce the order of the differential equations we perform the Fourier transformation as

$$R_n^{(l,r)}(p_y) = \int_{-\infty}^{+\infty} g_{1,2}^{(n)}(Y)\exp\left(\frac{i\ell_c}{\hbar\alpha}Y\widetilde{p}_y\right)dY \quad \text{(B6)}$$

and get the following set of equations:

$$i\alpha v_1^{(n)}\frac{dg_1^{(n)}}{dY} - (\varepsilon - \varepsilon_0^{(n)} - Y^2)g_1^{(n)} + \tilde{\Delta}g_2^{(n)} = 0;$$
$$i\alpha v_2^{(n)}\frac{dg_2}{dY} + (\varepsilon - \varepsilon_0^{(n)} - Y^2)g_2^{(n)} - \tilde{\Delta}g_1^{(n)} = 0; \quad \text{(B7)}$$

a. Transfer matrix in the Y-space.

Using Eq.(B7) and presenting the Fourier factors $g_{1,2}^{(n)}(Y)$ in the form

$$g_1^{(n)} = u_1^{(n)}(\zeta)\exp\{-i\left(\frac{v_2^{(n)}}{v_1^{(n)}+v_2^{(n)}}(\zeta^3/3 + \eta_n\zeta)\right)\}$$
$$g_2^{(n)} = u_2^{(n)}(\zeta)\exp\{+i\left(\frac{v_1^{(n)}}{v_1^{(n)}+v_2^{(n)}}(\zeta^3/3 + \eta_n\zeta)\right)\} \quad \text{(B8)}$$

together with a change of the variable

$$\zeta = Y[\frac{\ell_c\omega_c}{\alpha\overline{v}_n})]^{1/3}; \quad \overline{v}_n = \frac{v_1^{(n)}v_2^{(n)}}{v_1^{(n)}+v_2^{(n)}}$$

one gets the following parameterized set of equations

$$i\frac{du_1^{(n)}(\zeta)}{d\zeta} = +\overline{\gamma}_n\frac{v_2^{(n)}}{v_1^{(n)}+v_2^{(n)}}e^{+i\left(\frac{2}{3}\zeta^3+\eta_n\zeta\right)}u_2(\zeta)$$
$$i\frac{du_1^{(n)}(\zeta)}{d\zeta} = -\overline{\gamma}_n\frac{v_1^{(n)}}{v_1^{(n)}+v_2^{(n)}}e^{-i\left(\frac{2}{3}\zeta^3+\eta_n\zeta\right)}u_2(\zeta), \quad \text{(B9)}$$

where

$$\overline{\gamma}_n = \tilde{\Delta}[\frac{\ell_c\omega_c}{\alpha\overline{v}_n}]^{2/3}; \quad \eta_n = (\varepsilon_0^{(n)} - \varepsilon)[\frac{\ell_c\omega_c}{\alpha\overline{v}_n}]^{2/3}. \quad \text{(B10)}$$

We note here that analogous set of equations (with $v_1^{(n)} = v_2^{(n)} = v_F$) define the magnetic breakdown probability near touching points of classical orbits of an electron under a strong magnetic field as it was shown and analyzed in paper[24].

We assume $\gamma_n \ll 1$ and find the following solution of Eq.(B9) by the perturbation theory:

$$u_1^{(n)}(\zeta) = -i\overline{\gamma}_n\frac{v_2^{(n)}}{v_1^{(n)}+v_2^{(n)}}u_2^{(n)}(-\infty)\int_{-\infty}^{\zeta}d\chi e^{if(\chi)} +$$
$$u_1^{(n)}(-\infty)\Big[1 + (\overline{\gamma}_n\overline{w}_n)^2\int_{-\infty}^{\zeta}d\chi e^{if(\chi)}\int_{-\infty}^{\chi}d\chi' e^{-if(\chi')}\Big]$$
$$u_2^{(n)}(\zeta) = i\overline{\gamma}_n\frac{v_2^{(n)}}{v_1^{(n)}+v_1^{(n)}}u_1^{(n)}(-\infty)\int_{-\infty}^{\zeta}d\chi e^{-if(\chi)} +$$
$$u_2^{(n)}(-\infty)\Big[1 + (\overline{\gamma}_n\overline{w}_n)^2\int_{-\infty}^{\zeta}d\chi e^{-if(\chi)}\int_{-\infty}^{\chi}d\chi' e^{if(\chi')}\Big] \quad \text{(B11)}$$

where

$$f(\zeta) = \frac{\zeta^3}{3} + \eta_n\zeta;$$
$$\overline{w}_n = \frac{\sqrt{v_1^{(n)}v_2^{(n)}}}{v_1^{(n)}+v_2^{(n)}}; \quad \text{(B12)}$$

Taking $|\zeta| \gg 1$ one gets the transfer matrix

$$\hat{\tau_n} = \begin{pmatrix} 1 + (\overline{\gamma}_n\overline{w}_n)^2 a_2^{(n)} & i\overline{\gamma}_n\frac{v_2^{(n)}}{v_1^{(n)}+v_2^{(n)}}a_1^{(n)} \\ -i\overline{\gamma}_n\frac{v_1^{(n)}}{v_1^{(n)}+v_2^{(n)}}a_1^{(n)\star} & 1 + (\overline{\gamma}_n\overline{w}_n)^2 a_2^{(n)\star} \end{pmatrix} \quad \text{(B13)}$$

that couples constants $u_{1,2}^{(n)}(-\infty)$ in the solutions of Eq.(B9) at $\zeta < 0, -\zeta \gg 1$ and their asymptotic $u_{1,2}^{(n)}(+\infty)$ at $\zeta > 0, \zeta \gg 1$ as

$$\begin{pmatrix} u_1^{(n)}(+\infty) \\ u_2^{(n)}(+\infty) \end{pmatrix} = \hat{\tau}\begin{pmatrix} u_1^{(n)}(-\infty) \\ u_2^{(n)}(-\infty) \end{pmatrix} \quad \text{(B14)}$$

Here,

$$a_1^{(n)} \equiv a_1(\eta_n) = \int_{-\infty}^{+\infty} \exp\Big\{-i\big(\frac{\chi^3}{3}+\eta_n\chi\big)\Big\}d\chi = 2\pi \mathrm{Ai}\,(\eta_n)\,; \quad \text{(B15)}$$

and

$$a_2^{(n)} = \int_{-\infty}^{+\infty} d\chi \exp\Big\{-i\big(\frac{\chi^3}{3}+\eta_n\chi\big)\Big\} \times \int_{-\infty}^{\chi} d\tau \exp\Big\{+i\big(\frac{\chi^3}{3}+\eta_n\tau\big)\Big\}, \quad \text{(B16)}$$

where $\mathrm{Ai}\,(x)$ is the Airy function; one easily sees that $a_2 + a_2^\star = |a_1|^2$.

In the next subsection we calculate the asymptotic of Eq.(B6) at large $|\widetilde{p_y}|$ to use it later for matching the quasiclassical wave functions Eqs.(B3,B4) on the both sides of the degeneration point $p_y^{(n)}$.

b. Derivation of the transmission matrix that couples the semiclassical wave functions in the vicinity of the degeneration point.

Using Eqs.(B6,B8) one finds the wave functions in the momentum space as follows:

$$R_n^{(l)}(\overline{p}_y) = (\alpha\overline{v}_n)^{1/3}\int_{-\infty}^{+\infty} u_1^{(n)}(\zeta)\exp\Big\{-i\Big[\frac{v_2^{(n)}}{v_1^{(n)}+v_2^{(n)}}\frac{\zeta^3}{3} + \Big(\frac{v_2^{(n)}}{v_1^{(n)}+v_2^{(n)}}\eta_n - \frac{1}{\hbar}(\frac{\overline{v}_n\ell_c^2}{\alpha^2\omega_c})^{1/3}\widetilde{p_y}\Big)\zeta\Big]\Big\}d\zeta$$

$$R_n^{(r)}(\overline{p}_y) = (\alpha\overline{v}_n)^{1/3}\int_{-\infty}^{+\infty} u_2^{(n)}(\zeta)\exp\Big\{+i\Big[\frac{v_2^{(n)}}{v_1^{(n)}+v_2^{(n)}}\frac{\zeta^3}{3} + \Big(\frac{v_2^{(n)}}{v_1^{(n)}+v_2^{(n)}}\eta_n + \frac{1}{\hbar}(\frac{\overline{v}_n\ell_c^2}{\alpha^2\omega_c})^{1/3}\widetilde{p_y}\Big)\zeta\Big]\Big\}d\zeta \quad \text{(B17)}$$

We perform the integration over ζ by the steepest descent method at $|p_y - p_y^{(n)}| \gg (\alpha^2\ell_c\omega_c/\overline{v}_n)^{1/3}(\hbar/\ell_c)$.

As one sees from Eq.(B17) the saddle points are

$$\zeta_\pm^{(1)} = \pm\frac{(\ell_c\omega_c)^{1/3}}{(\alpha\overline{v}_n)^{1/3}}\sqrt{\varepsilon - \varepsilon_0^{(n)} + v_n^{(l)}p_y}; \quad \text{(B18)}$$

for the integral in the expression for $R_n^{(l)}$ and

$$\zeta_\pm^{(2)} = \pm\frac{(\ell_c\omega_c)^{1/3}}{(\alpha\overline{v}_n)^{1/3}}\sqrt{\varepsilon - \varepsilon_0^{(n)} - v_n^{(r)}p_y}; \quad \text{(B19)}$$

for the integral in the expression for $R_n^{(r)}$.

Using Eqs.(B17-B19) one finds the asymptotic of $R_n^{(l,r)}$ at $p_F \gg |p_y - p_y^{(n)}| \gg (\alpha^2/v)^{1/3}$ (here, v_F and p_F are the Fermi velocity and momentum) as follows:

$$p_y - p_y^{(n)} < 0,$$

$$R_n^{(l)}(p_y) \propto \exp\Big[-\frac{2}{3}\frac{\ell_c\omega_c\big(\widetilde{\varepsilon}_n^{(l)}(p_y)-\varepsilon\big)^{3/2}}{\alpha v_n^{(l)}}\Big];$$

$$R_n^{(r)}(p_y) = \frac{\sqrt{\pi\alpha v_n^{(r)}}}{\big(\varepsilon - \widetilde{\varepsilon}_n^{(r)}(p_y)\big)^{1/4}} \times\Big\{u_2^{(n)}(-\infty)\exp\Big[i\Big(\frac{2}{3}\frac{\ell_c\omega_c\big(\varepsilon-\widetilde{\varepsilon}_n^{(r)}(p_y)\big)^{3/2}}{\alpha v_n^{(r)}}+\frac{\pi}{4}\Big)\Big] + u_2^{(n)}(+\infty)\exp\Big[-i\Big(\frac{2}{3}\frac{\ell_c\omega_c\big(\varepsilon-\widetilde{\varepsilon}_n^{(r)}(p_y)\big)^{3/2}}{\alpha v_n^{(r)}}+\frac{\pi}{4}\Big)\Big]\Big\} \quad \text{(B20)}$$

$$p_y - p_y^{(n)} > 0,$$

$$R_n^{(l)}(p_y) = \frac{\sqrt{\pi\alpha v_n^{(l)}}}{\big(\varepsilon - \widetilde{\varepsilon}_n^{(l)}(p_y)\big)^{1/4}} \times\Big\{u_1^{(n)}(-\infty)\exp\Big[-i\Big(\frac{2}{3}\frac{\ell_c\omega_c\big(\varepsilon-\widetilde{\varepsilon}_n^{(l)}(p_y)\big)^{3/2}}{\alpha v_n^{(l)}}-\frac{\pi}{4}\Big)\Big] + u_1^{(n)}(+\infty)\exp\Big[+i\Big(\frac{2}{3}\frac{\ell_c\omega_c\big(\varepsilon-\widetilde{\varepsilon}_n^{(l)}(p_y)\big)^{3/2}}{\alpha v_n^{(l)}}-\frac{\pi}{4}\Big)\Big]\Big\};$$

$$R_n^{(r)}(p_y) \propto \exp\Big[-\frac{2}{3}\frac{\ell_c\omega_c\big(\widetilde{\varepsilon}_n^{(r)}(p_y)-\varepsilon\big)^{3/2}}{\alpha v_n^{(r)}}\Big], \quad \text{(B21)}$$

where $\widetilde{\varepsilon}_n^{(l,r)}(p_y) = \varepsilon_0^{(n)} \mp v_n^{(l,r)}(p_y - p_y^{(n)})$ are the edge state energies expanded near the degenerate point $p_y^{(n)}$.

Matching the wave functions Eqs.(B20, B21) and the quasiclassical wave functions Eqs.(B3,B4) in the overlapping region $p_F \gg |p_y - p_y^{(n)}| \gg (\ell_c\omega_c\alpha^2/v_F)^{1/3}(\hbar/\ell_c)$ we obtain

$$p_y - p_y^{(n)} < 0$$

$$C_1^{(n)} = \sqrt{\alpha\pi v_n^{(r)}}e^{-i\pi/4}u_2^{(n)}(+\infty);$$

$$C_2^{(n)} = \sqrt{\alpha\pi v_n^{(r)}}e^{+i\pi/4}u_2^{(n)}(-\infty);$$

$$p_y - p_y^{(n)} > 0$$

$$B_1^{(n)} = \sqrt{\alpha\pi v_n^{(l)}}e^{-i\pi/4}u_1^{(n)}(+\infty);$$

$$B_2^{(n)} = \sqrt{\alpha\pi v_n^{(l)}}e^{+i\pi/4}u_1^{(n)}(-\infty); \quad \text{(B22)}$$

The other constants one may put equal to zero.

Using Eq.(B22) and Eqs.(B13,B14) one finds the transmission matrix that couples the amplitudes of the incoming, $B_2^{(n)}$, $C_1^{(n)}$, and outgoing, $B_1^{(n)}$, $C_2^{(n)}$, quasiclassical wave functions Eqs.(B3,B4) on the both sides of the region around $p_y^{(n)}$

$$\begin{pmatrix} B_1^{(n)} \\ C_2^{(n)} \end{pmatrix} = \hat{t}_n \begin{pmatrix} B_2^{(n)} \\ C_1^{(n)} \end{pmatrix} \quad \text{(B23)}$$

where

$$\hat{t}_n = e^{i\Theta}\begin{pmatrix} -1+\frac{(\overline{\gamma}_n\overline{w}_n)^2}{2}|a_1^{(n)}|^2 & \overline{\gamma}_n\overline{w}_n a_1^{(n)} \\ \overline{\gamma}_n\overline{w}_n a_1^{(n)} & 1-\frac{(\overline{\gamma}_n\overline{w}_n)^2}{2}|a_1^{(n)}|^2 \end{pmatrix} \quad \text{(B24)}$$

and $\Theta = (\overline{\gamma}_n\overline{w}_n)^2\, Im\{a_2^{(n)}\} - \pi/2$. Equation Eq.(B24) is written with the accuracy of the second order of $\overline{\gamma}_n$ while parameters $\overline{\gamma}_n$, $\overline{w}_n$ are defined in Eq.(B10).

The transmission matrix $\hat{t}_n$ couples the quasiclassical wave functions Eqs.(B3,B4) on the both sides of any point of intersection of the two edge state dispersion laws, e.g., for the case that the energy is in the vicinity of $\varepsilon_0^{(1)}$ (see Fig.5) these regions are $-\infty \le p_y \lesssim p_y^{(I)} - (\alpha^2/\overline{v}_F)^{1/3}$, $p_y^{(I)} + (\alpha^2/\overline{v}_F)^{1/3} \lesssim p_y \lesssim p_y^{(II)} - (\alpha^2/\overline{v}_F)^{1/3}$.

In the next section we the find electron wave functions at $x \to -\infty$ and $x \to +\infty$ that allows to find the probability of electron transmission through the point contact under considerations.

3. The matrix of transmission through the point contact from $p_y \to -\infty$ to $p_y \to +\infty$.

To find the probability for an electron to pass through the point contact one firstly needs to know connections between the coefficients in the incoming and outgoing quasiclassical wave functions at $p_y \to \pm\infty$. As it follows from Eqs.(B3,B4), in these regions the functions are

$$p_y \to -\infty; \qquad R_n^{(l)}(p_y) = \frac{1}{\sqrt{p_x^{(n)}}}$$
$$\times\left[C_{in}^{(l,n)}\exp\left(i\frac{p_x^{(n)}p_y}{p_1^2}\right) + C_{out}^{(l,n)}\exp\left(-i\frac{p_x^{(n)}p_y}{p_1^2}\right)\right]$$
$$p_y \to +\infty; \qquad R_n^{(r)}(p_y) = \frac{1}{\sqrt{p_x^{(n)}}}$$
$$\times\left[C_{out}^{(r,n)}\exp\left(i\frac{p_x^{(n)}p_y}{p_1^2}\right) + C_{in}^{(r,n)}\exp\left(-i\frac{p_x^{(n)}p_y}{p_1^2}\right)\right] \quad \text{(B25)}$$

where $p_x^{(n)} = \sqrt{2m(E-\hbar\omega_H(n+1/2)}$, and $p_1^2 = m\hbar\omega_1$; $C_{in}^{(n)}$, $C_{in}^{(n)}$ and $C_{out}^{(n)}$, $B_{out}^{(n)}$ are the amplitudes of the incoming and outgoing wave functions normalized to the unity flux. While writing the above equation we took into account that in the limiting regions the electron energy $E_n(p_y) \to \hbar\omega_H(n+1/2)$.

We start from the case that the electron energy is in the vicinity of $\varepsilon_0^{(1)}$ as is shown in Fig.5 and hence there are two points $p_y^{(I)}$ and $p_y^{(II)}$ at which the quasiclassical trajectories undergo topological transitions under a change of the electron energy. The quasiclassical trajectories at the electron energy above this point, $\varepsilon > \varepsilon_0^{(1)}$, are presented in Fig.5b2.

Matching quasiclassical wave functions Eq.(B25) with the help od the transfer matrix Eq.(B23,B24), and taking into account the quasiclassical phase gains between the degeneracy points $p_y^{(I,II)}$ one finds the coupling between the outgoing coefficients $C_{out}^{(r,0)}$, $C_{out}^{(r,1)}$ and the incoming ones $C_{in}^{(l,0)}$, $C_{in}^{(r,1)}$ as follows:

$$C_{out}^{(r,n-1)} = t_L\frac{1-|r_n|^2\exp\{i\chi_+\}}{1-|t_L|^2|r_n|^2\exp\{i\chi_+\}}C_{in}^{(l,n-1)} - r_L\frac{t_n^\star\exp\{i\chi_+\}}{1-|t_L|^2|r_n|^2\exp\{i\chi_+\}}C_{in}^{(l,n)}$$
$$C_{out}^{(r,n)} = r_L^\star\frac{t_n^\star\exp\{i\chi_+\}}{1-|t_L|^2|r_n|^2\exp\{i\chi_+\}}C_{in}^{(l,n-1)} + t_L^\star\frac{t_n^\star\exp\{i\chi_+\}}{1-|t_L|^2|r_n|^2\exp\{i\chi_+\}}C_{in}^{(l,n)} \quad \text{(B26)}$$

where $n = 1$ and

$$|t_L|^2 = \frac{\ell_c\omega_c\pi|\tilde{\Delta}|^2}{\alpha v_1\sqrt{\varepsilon-\varepsilon_0^{(0)}}} = \frac{\pi|\Delta|^2}{\hbar\omega^\star V_1 P_0^\star}$$

is the standard Landau-Zener probabilities of the interband transitions that take place at $p_y = 0$ where two semiclassical trajectories approach each other, $V_1 = dE_1/dp_y$,$\omega_H^\star = eH\hbar/m^\star c$, $m^\star = m/\alpha^2$, while $P_0^\star = \sqrt{2m^\star(E-E_0^{(0)})}$ and χ_+ is the phase gain along the large close orbit in Fig.5b (which is closed via the small closed orbits, the latter being neglected), $|r_n| = 1 - \frac{|t_1(\eta_n|^2}{2}|$ and

$$t_1 = -i\exp\{i\Theta\}\overline{\gamma}_1\overline{w}_1 a_1 \quad \text{(B27)}$$

Here γ_1, $\overline{w}_1$, a_1, η_1 are defined in Eqs.(B10,B12,B15) in which $v_{1,2}^{(1)} \equiv v_{0,1} = d\overline{\varepsilon}_{0,1}(p_y)/dp_y$ are the velocities of the edge states $n = 0$ and $n = 1$.

As in the case under consideration $E - E_0^{(0)} \sim \hbar\omega_H$ and $V_1 \sim \sqrt{\hbar\omega_H/m}$ one has

$$|t_L|^2/|t_n|^2 \sim (\frac{\alpha v_F}{\ell_c\omega_c})^{1/3}/\sqrt{\varepsilon-\varepsilon_0^{(0)}} \sim \alpha^{1/3} \ll 1$$

and hence one may approximately write

$$C_{out}^{(r,n-1)} \approx -t_n^\star\exp\{i\chi_+\}C_{in}^{(n)}$$
$$C_{out}^{(r,n)} \approx +t_n\exp\{i\chi_+\}C_{in}^{(n-1)}; \quad \text{(B28)}$$

From here it follows that in the first approximation in $\overline{\gamma}_n \ll 1$ the probability for an electron to pass from $p_y \to -\infty$ to $p_y \to +\infty$ is approximately equal to $|t_n|$ for each incoming open mode 0 and 1. Considering the electron energy at higher values and checking possible semiclassical paths of transmission one finds that an analogous rule is correct for any number of incoming open modes which may be written as follows:

$$|C_{out}^{(r,k)}|^2 = D_k^{n-k}|C_{in}^{(l,n-k)}|^2; \quad k = 0,1,...n \quad \text{(B29)}$$

where $C_{in}^{(l,n}$ and $C_{out}^{(r,n)}$ are the amplitudes of the incoming (at $p_y \to -\infty$) and the outgoing (at $p_y \to +\infty$) semiclassical wave functions Eq.(B25), respectively, n is the maximal quantum number of the incoming (outgoing) modes

present at a given energy ε (e.g., $n=2$ for the case that $\varepsilon \approx \varepsilon_0^{(2)}$, see Fig5). The transmission probability is

$$D_k^{n-k} = |\overline{\gamma}_k^{(n-k)} \overline{w}_k^{(n-k)} a_1(\eta_n^{(n-k)})|^2; \quad k = 0, 1, ...n \tag{B30}$$

where $\overline{\gamma}_k^{(n-k)} \equiv \overline{\gamma}_n$, $\overline{w}_k^{(n-k)} \equiv \overline{w}_n$, $\eta_n^{(n_m-n)} \equiv \eta_n$ are presented in Eqs.(B10,B12) in which the Landau numbers of the velocities are now explicitly written:

$$\overline{\gamma}_k^{(n-k)} = [\frac{\ell_c \omega_c}{\alpha \overline{v}_n^{(n-k)}}]^{2/3} \Delta_n; \quad \overline{v}_k^{(n_m-k)} = \frac{v_k v_{n-k}}{v_k + v_{n-k}};$$
$$\eta_k^{(n-k)} = [\frac{\ell_c \omega_c}{\alpha \overline{v}_k^{(n-k)}}]^{2/3} (\varepsilon_0^{(n)} - \varepsilon); \quad \overline{w}_k^{(n-k)} = \frac{\sqrt{v_k v_{n-k}}}{v_k + v_{n-k}} \tag{B31}$$

Using Eq.(B30) and Eq.(B31) at $n = k = 0$ one gets Eqs.(10,11) of the main text.

Appendix C: Derivation of Eq.(12) of the main text.

1 step, subsection A. Using the semiclassical wave functions in the momentum space (found in Section II) we find the electron wave functions in the coordinate space which are the solution of the Shr odinger Eq.(1) written in theLandau gauge $\mathbf{A} = (0, Hx, 0)$ *in which the project momentum* p_x *does not conserve and hence these functions can not be directly used to describe the electron transport in terms of the incoming and outgoing electrons.*

2 step. In subsection B we re-write the electron wave functions in the form that is the solution of the Shrödinger equation in which the gauge $\mathbf{A} = (-Hy, 0, 0)$ *is used that allows to use the Landauer-Büttiker approach and find Eq.(12) of the main text.*

1. Asymptotic of the electron wave functions at $x \gg R_L$ and the gauge $\mathbf{A} = (0, Hx, 0)$.

Equation (B29)allows to connect the asymptotic of the electron wave functions both in the momentum and coordinate spaces for any number of incoming modes n.

Taking the quasiclassical functions Eqs.(B3,B4) in the region $|p_y| \gg (eH/c)R_L = p_E = \sqrt{2mE}$ (that is far from the barrier where the electron spectrum is discrete, $E_n = \hbar\omega(n+1/2)$), one finds the Fourier factor Q (see Eq.(**??**) as follows:

$$Q^{(l,r)}(x, p_y) = \sum_{\{n\}} \frac{1}{\sqrt{p_x^{(n)}}} \times$$
$$\left[C_{in}^{(l,r;n)} \exp\left(i\frac{p_x^{(n)} p_y}{p_1^2}\right) + C_{out}^{(l,r;n)} \exp\left(-i\frac{p_x^{(n)} p_y}{p_1^2}\right)\right]$$
$$\times \exp\left[-\frac{(x + cp_y/eh)^2}{2\ell_c^2}\right] H_n(\frac{(x + cp_y/eh)}{\ell_c}) \tag{C1}$$

where the sum is over all edge state modes n present at a given electron energy ε; $H_n(x)$ is the Hermite polynomial; the superscripts (l) and (r) denote the regions $p_y < 0$ and $p_y > 0$, respectively. While writing Eq.(C1) we have taken into account Eq.(A3) and the fact that $R_n^{(r)} \approx 0$ at $p_y < 0$, and $R_n^{(l)} \approx 0$ at $p_y > 0$.

Inserting Eq.(C1) in Eq.(2)of the main text one finds the asymptotic of the wave function $\Psi(x,y)^{(l,r)}$ at $|x| \gg R_L$ in the left part (l), $x < 0$, and the right part (r), $x < 0$, of the system as follows:

$$\Psi^{(l)}(x, y) =$$
$$\exp\{-i\frac{eH\hbar}{c}xy\} \sum_{\{n\}} \left[C_{in}^{(l,n)} \exp\left(-i\frac{eH}{cp_1^2}p_x^{(n)}x\right) \times \right.$$
$$\int_{-\infty}^{+\infty} \exp\{-q^2/2\sigma\} \exp\{i\left(\frac{p_x^{(n)}}{p_1^2} + \frac{y}{\hbar}\right) q\} H_n(\frac{q}{\sqrt{\sigma}}) dq$$
$$+ C_{out}^{(l,n)} \exp\left(-i\frac{eH}{cp_1^2}p_x^{(n)}x\right) \int_{-\infty}^{+\infty} \exp\{-q^2/2\sigma\}$$
$$\left. \times \exp\{-i\left(\frac{p_x^{(n)}}{p_1^2} - \frac{y}{\hbar}\right) q\} H_n(\frac{q}{\sqrt{\sigma}}) dq\right] \tag{C2}$$

and

$$\Psi^{(r)}(x, y) =$$
$$\exp\{-i\frac{eH\hbar}{c}xy\} \sum_{\{n\}} \left[C_{out}^{(r,n)} \exp\left(-i\frac{eH}{cp_1^2}p_x^{(n)}x\right) \times \right.$$
$$\int_{-\infty}^{+\infty} \exp\{-q^2/2\sigma\} \exp\{i\left(\frac{p_x^{(n)}}{p_1^2} + \frac{y}{\hbar}\right) q\} H_n(\frac{q}{\sqrt{\sigma}}) dq$$
$$+ C_{in}^{(r,n)} \exp\left(-i\frac{eH}{cp_1^2}p_x^{(n)}x\right) \int_{-\infty}^{+\infty} \exp\{-q^2/2\sigma\}$$
$$\left. \times \exp\{-i\left(\frac{p_x^{(n)}}{p_1^2} - \frac{y}{\hbar}\right) q\} H_n(\frac{q}{\sqrt{\sigma}}) dq\right] \tag{C3}$$

where $p_x^{(n)} = \sqrt{2m[E - \hbar\omega_H(n+1/2)]}$, $p_1^2 = m\hbar\omega_1$, $\sigma = e\hbar H/c$.

In the next section we show that these wave functions may be presented in the form convenient for calculations of the current flux through the point contact.

2. Gauge change in the presentation of the found wave functions.

The found wave functions Eq.(C2,C3), are the solutions of the Schrödinger equation Eq.(1) of the main text in which the gauge $\mathbf{A} = (0, Hx, 0)$ *is used. In this gauge the* p_x*-projection of the momentum of the incoming and outgoing edge states does not conserve and hence one can not directly use these functions to find the current flowing along the point contact. In this subsection we recast the wave functions Eq.(C2,**??**) into the form that corresponds to the gauge* $\mathbf{A} = (-Hy, 0, 0)$ *in which* p_x *conserves.*

a. Derivation of the equality that allows the gauge transformation.

We use the generating function of the Hermite polynomials (see, e.g.,[?])

$$\exp\{-s^2+2sq\}=\sum_{k=0}^{\infty}\frac{s^k}{k!}H_k(q); \tag{C4}$$

Multiplying the both sides of it by $\exp\{-q^2+i\widetilde{y}q\}$ and integrating with respect to q one gets

$$\int_{\infty}^{\infty}\exp\{-q^2+i\widetilde{y}q\}\exp\{-s^2+2sq\}dq$$
$$=\sum_{k=0}^{\infty}\frac{t^k}{k!}\int_{\infty}^{\infty}\exp\{-q^2+i\widetilde{y}q\}H_k(q)dq; \tag{C5}$$

Integrating the left-hand side one easily finds

$$\sum_{k=0}^{\infty}\frac{s^k}{k!}\int_{\infty}^{\infty}\exp\{-q^2+i\widetilde{y}q\}H_k(q)dq$$
$$=\sqrt{2\pi}e^{-\widetilde{y}^2/2}\exp\{-(is)^2+2(is)\widetilde{y}\}; \tag{C6}$$

Applying Eq.(C4) to the right-hand side of this equation one gets the following:

$$\sum_{k=0}^{\infty}\frac{s^k}{k!}\Big\{\int_{\infty}^{\infty}\exp\{-q^2+i\widetilde{y}q\}H_k(q)dq$$
$$-i^k\sqrt{2\pi}H_k(\widetilde{y})\Big\}=0; \tag{C7}$$

As s is arbitrary one gets the following equation:

$$\int_{\infty}^{\infty}\exp\{-q^2+i\widetilde{y}q\}H_k(q)dq=i^k\sqrt{2\pi}H_k(\widetilde{y})\} \tag{C8}$$

b. Wave functions of the incoming electrons and those scattered by the lateral junction in which p_x conserves.

Now applying the obtained equality Eq.(C8) to Eqs.(C2,C3) we get the wave functions as follows:

$$x\to-\infty;$$
$$\Psi^{(l)}(x,y)=\sqrt{2\pi\sigma}e^{-i(eH/\hbar c)xy}\times$$
$$\sum_{\{n\}}i^n\Big[C_{in}^{(l,n)}\exp\{-i\frac{p_x^{(n,\star)}x}{\hbar}\}\exp\{-\frac{y_{n,+}^2}{2\ell_c^2}\}H_n(\frac{y_{n,+}}{\ell_c})$$
$$+C_{out}^{(l,n)}\exp\{+i\frac{p_x^{(n,\star)}x}{\hbar}\}\exp\{-\frac{y_{n,-}^2}{2\ell_c^2}\}H_n(\frac{y_{n,-}}{\ell_c})\Big] \tag{C9}$$

and

$$x\to+\infty;$$
$$\Psi^{(r)}(x,y)=\sqrt{2\pi\sigma}e^{-i(eH/\hbar c)xy}\times$$
$$\sum_{\{n\}}i^n\Big[C_{out}^{(r,n)}\exp\{-i\frac{p_x^{(n,\star)}x}{\hbar}\}\exp\{-\frac{y_{n,+}^2}{2\ell_c^2}\}H_n(\frac{y_{n,+}}{\ell_c})$$
$$+C_{in}^{(r,n)}\exp\{+i\frac{p_x^{(n,\star)}x}{\hbar}\}\exp\{-\frac{y_{n,-}^2}{2\ell_c^2}\}H_n(\frac{y_{n,-}}{\ell_c})\Big] \tag{C10}$$

where $p_x^{(n,\star)}=\sqrt{2m^\star[E-\hbar\omega_H(n+1/2)]}$, $m^\star=m/\alpha^2$ is the re-normalized mass and $y_{n,\pm}=y\pm cp_x^{n,\star}/eH$ while the constant factors at the incoming, $C_{in}^{(r,n)}$, and outgoing wave functions, $C_{out}^{(r,n)}$, (which are normalized to the unity flux) are connected to one another by the relations Eqs.(B29,B30,B31).

The wave functions inside the square brackets are solutions of Schrödinger's equation Eq.(1) at $|x|\gg R_L$ in which the gauge of the vector potential is changed to $\mathbf{A}=(-Hx,0,0)$ that conserves the projection of the electron momentum p_x parallel to the longitudinal direction of the junction.

Using Eqs.(C9,C10)together with Eq.(B29) one finds the current flowing along the junction as follows:

$$I(V)=\frac{2e}{h}\sum_{n=0}^{\infty}\sum_{k=0}^{n}\int_{-\infty}^{\infty}dED_n^{n-k}\big(E-E_n^{n-k}(V)\big) \tag{C11}$$
$$[f(E+eV/2)-f(E-eV/2)]\ ,$$

where $E_n^{n-k}(V)$ is the energy of degeneration of the left and right edge states under applied voltage drop V, that is $E_n^{n-k}(V)\equiv E_n^{(l)}(p_y)+eV/2=E_k^{(r)}(p_y)-eV/2$.

Eq.(12) of the main text is a simplified form of Eq.(C11).